

31 **Abstract**

32 Infection with SARS-CoV-2 has caused a pandemic of unprecedented dimensions. SARS-CoV-2
33 infects airway and lung cells causing viral pneumonia. The importance of type I interferon (IFN)
34 production for the control of SARS-CoV-2 infection is highlighted by the increased severity of
35 COVID-19 in patients with inborn errors of type I IFN response or auto-antibodies against IFN- α .
36 Plasmacytoid dendritic cells (pDCs) are a unique immune cell population specialized in
37 recognizing and controlling viral infections through the production of high concentrations of type I
38 IFN. In this study, we isolated pDCs from healthy donors and showed that pDCs are able to
39 recognize SARS-CoV-2 and rapidly produce large amounts of type I IFN. Sensing of SARS-CoV-
40 2 by pDCs was independent of viral replication since pDCs were also able to recognize UV-
41 inactivated SARS-CoV-2 and produce type I IFN. Transcriptional profiling of SARS-CoV-2 and
42 UV-SARS-CoV-2 stimulated pDCs also showed a rapid type I and III IFN response as well as
43 induction of several chemokines, and the induction of apoptosis in pDCs. Moreover, we modeled
44 SARS-CoV-2 infection in the lung using primary human airway epithelial cells (pHAEs) and
45 showed that co-culture of pDCs with SARS-CoV-2 infected pHAEs induces an antiviral response
46 and upregulation of antigen presentation in pHAE cells. Importantly, the presence of pDCs in the
47 co-culture results in control of SARS-CoV-2 replication in pHAEs. Our study identifies pDCs as
48 one of the key cells that can recognize SARS-CoV-2 infection, produce type I and III IFN and
49 control viral replication in infected cells.

50

51

52 **Importance**

53 Type I interferons (IFNs) are a major part of the innate immune defense against viral
54 infections. The importance of type I interferon (IFN) production for the control of SARS-CoV-2
55 infection is highlighted by the increased severity of COVID-19 in patients with defects in the type
56 I IFN response. Interestingly, many cells are not able to produce type I IFN after being infected
57 with SARS-CoV-2 and cannot control viral infection. In this study we show that plasmacytoid
58 dendritic cells are able to recognize SARS-CoV-2 and produce type I IFN, and that pDCs are able
59 to help control viral infection in SARS-CoV-2 infected airway epithelial cells.

60 **Introduction**

61 Infection with SARS-CoV-2 in humans has caused a pandemic of unprecedented dimensions. In
62 the United States, more than 31 million people have tested positive for infection and more than
63 550,000 have died as of April 2021. SARS-CoV-2 infects airway epithelial cells and Type 2
64 pneumocytes causing fever, dry cough, and shortness of breath. While most patients experience
65 mild to moderate disease, some progress to more severe disease, including pneumonia and acute
66 respiratory failure. Severe cases of COVID-19 can result in lung damage, low blood oxygen levels,
67 and death^{1,2}.

68

69 Type I and III IFNs are a major part of the innate immune defense against viral infections³. One
70 characteristic of coronavirus infections including SARS-CoV-2 is the low induction of type I IFN in
71 the host⁴⁻⁶. The reduced type I IFN production from infected cells is caused by both lack of
72 recognition of the viral RNA by pathogen recognition receptors, and the IFN antagonist function
73 of several viral non-structural proteins (nsp; as reviewed in^{7,8}). Early reports detected low levels
74 of type I IFN in the blood of COVID-19 patients⁴. However, transcriptional analysis of
75 bronchoalveolar lavage (BAL) or peripheral blood of COVID-19 patients detected an early type I
76 IFN signature⁹⁻¹¹. The importance of type I IFN production for the control of SARS-CoV-2 infection
77 is highlighted by the increased severity of COVID-19 in patients with inborn errors of type I IFN
78 response, as well as patients presenting with auto-antibodies against IFN- α ^{12,13}. Moreover, IFN-
79 2 α treatment of COVID-19 patients with inborn errors of type I IFN response, as well as early
80 administration of IFN- α 2 to COVID-19 patients reduced in hospital mortality^{14,15}.

81

82 Plasmacytoid dendritic cells (pDCs) are a unique immune cell population specialized in
83 recognizing and controlling viral infections through the production of high concentrations of type I

84 IFN^{16,17}. pDCs have unique features that enable their unparalleled antiviral response. They
85 express pattern recognition receptors like TLR7 or TLR9¹⁸, which allow pDCs to sense viral RNA
86 or DNA even in the absence of viral infection or replication¹⁹. They constitutively express IRF-7,
87 the master transcription factor for interferon (IFN)- α , which enables rapid production and secretion
88 of IFN- α ^{16,17}. Both human and murine pDCs can sense SARS-CoV and the murine coronavirus
89 MHV-A59 respectively. pDCs can sense these coronaviruses through TLR7 and produce high
90 concentrations of IFN- α ^{20,21}. pDCs numbers are reduced in the blood of COVID-19 patients⁹.
91 However, increased numbers of pDCs are found in the BAL of mild COVID-19 patients in contrast
92 to severe COVID-19 patients which have reduced numbers of pDCs in BAL¹⁰. Network analyses
93 of single-cells RNA seq of COVID-19 patients showed an association between apoptosis in pDCs
94 and disease severity²². Despite these findings, we still lack studies that address the contribution
95 of pDCs to SARS-CoV-2 control in the airways.

96

97 Primary human airway epithelial cell cultures are permissive to SARS-CoV-2 infection, and have
98 been used for both short and long term modelling of infection. Ciliated cells and goblet cells are
99 permissive to infection while SARS-CoV-2 has not been detected on basal and club cells²³. Our
100 previous studies have shown that human airway epithelial cell cultures (pHAE) are unable to
101 produce a type I or III IFN response after infection with SARS-CoV-2²⁴. Similarly, Lieberman et al
102 observed no induction of interferon stimulated genes (ISGs) after 3 days of SARS-CoV-2 infection
103 in pHAEs²⁵. A delayed type I IFN response is observed in pHAEs after 7 days of infection and
104 positively correlates with the levels of replication of SARS-CoV-2²⁶, which is recognized by pHAE
105 cells through MDA-5²⁷. Importantly, in contrast to SARS-CoV, SARS-CoV-2 is susceptible to type
106 I and III IFN inhibition^{28,29}. Pre- or post-treatment of pHAEs with IFN- β or IFN- λ was able to reduce
107 SARS-CoV-2 replication, suggesting that if an IFN response can be elicited, it is effective in
108 controlling SARS-CoV-2 infection²⁴.

109 In this study, we tested the ability of pDCs to sense SARS-CoV-2. pDCs isolated from healthy
110 donors recognized SARS-CoV-2 and rapidly produced large concentrations of IFN- α . Sensing of
111 SARS-CoV-2 by pDCs was independent of viral replication. We observed that pDCs can
112 recognize UV-inactivated SARS-CoV-2 and produce type I IFN with similar kinetics.
113 Transcriptional profiling of SARS-CoV-2 and UV-SARS-CoV-2 showed a swift type I and III IFN
114 signature after 12h stimulation. Moreover, we observed the induction of several chemokines, pro-
115 inflammatory cytokines and the induction of apoptosis in pDCs. To test if type I IFN production by
116 pDCs was able to control viral replication we modeled SARS-CoV-2 infection in the lung using
117 primary human airway epithelial cells (pHAEs) and showed that co-culture of pDCs with SARS-
118 CoV-2 infected pHAEs induces an antiviral response and upregulation of antigen presentation in
119 pHAE cells. Importantly, the presence of pDCs in the co-culture results in control of SARS-CoV-
120 2 replication in pHAEs. Overall, our study identifies pDCs as a key cells that recognize SARS-
121 CoV-2 infection and produce type I and III IFN that can control viral replication in airway cells.

122 **Materials and Methods**

123 **Viruses and cells.** The infectious clone SARS-CoV-2 (icSARS-CoV-2) was kindly provided to
124 us by Dr. Vineet Menachery (UTMB)³⁰. Viral titers were determined by plaque assay or focus-
125 forming assay on VeroE6 cells (ATCC). VeroE6 cells were cultured in complete DMEM medium
126 consisting of 1x DMEM (Corning Cellgro), 10% FBS, 25 mM HEPES Buffer (Corning Cellgro), 2
127 mM L-glutamine, 1mM sodium pyruvate, 1x Non-essential Amino Acids, and 1x antibiotics. Viral
128 stocks were titered on VeroE6 cells and stored at -80°C until use.

129
130 **Plasmacytoid dendritic cell isolation.** Deidentified human blood from healthy individuals was
131 collected with the approval of the Internal Review Board (IRB) of Emory University number
132 IRB00045821. PBMCs were obtained by Ficoll-Hypaque density gradient centrifugation. pDCs
133 were further purified by magnetic sorting with human Diamond Plasmacytoid dendritic-cell
134 isolation kit II (Miltenyi Biotec). Purity of cell preparation was assessed by flow cytometry and for
135 all donors was more than 90%.

136
137 **Plasmacytoid dendritic cell stimulation.** 4×10^4 pDCs were infected with SARS-CoV-2 (MOI=1)
138 or stimulated with medium, UV inactivated SARS-CoV-2 (MOI=1) or CpG A (6ug/ml). After one-
139 hour medium was replaced and cells were incubated at 37°C. After 12hr cell were collected and
140 frozen for RNA isolation and after 24h supernatants were collected and frozen for ELISA
141 measurements.

142
143 **Generation of primary human airway epithelial cells.** pHAE cultures were generously provided
144 by Dr. C. U. Cotton (Case Western Reserve University) and cultured as described previously³¹.
145 Briefly, bronchial lung specimens were seeded on Transwell Permeable Support Inserts (Costar-

146 Corning) and cultured until confluent. Specimens were then transferred to an air/liquid interface
147 and differentiated for 2-3 weeks. Cultures were maintained in DMEM/Ham's F-12 medium
148 supplemented with 2% Ultrosor G (Pall Corp., France), until all wells had TEER measurements
149 greater than 1000 Ω and deemed ready for use.

150

151 **Co-culture of HAE and pDC cells.** pDCs were isolated as described above, then stimulated for
152 3 hours in complete RPMI supplemented with; medium, CpG A (ODN2216 at 6 μ g/ml), UV
153 inactivated SARS-CoV-2 (MOI=1) at 37°C. During the 3 hour stimulation, differentiated pHAE
154 cultures were infected; the apical side of the pHAE culture was washed 3 times with PBS, then
155 SARS-CoV-2 (MOI=1) was allowed to adsorb for 1 hour at 37°C. After adsorption, the apical side
156 was washed 3 times with PBS to remove excess virus. The basolateral media was then replaced
157 with fresh media containing the stimulated pDCs, medium only, or IFN β (100 IU/mL). Cells were
158 co-cultured for up to 72 hours, with no disturbance of the basolateral media. To collect viral
159 supernatant, PBS was added to the apical side and incubated for 30 minutes at 37°C.

160

161 **Focus-forming Assays.** To measure SARS-CoV-2 viral burden, supernatant from infected cells
162 was serially diluted (10-fold dilutions) in serum free RPMI. Virus dilutions were overlaid on VeroE6
163 cells and incubated with a methylcellulose overlay (0.85% methylcellulose in 2X DMEM) for 48
164 hours at 37°C. Methylcellulose was removed, cells were then fixed with 2%-PFA and
165 permeabilized with 0.1% bovine serum albumin (BSA)-Saponin in PBS. Permeabilized cell
166 monolayers were incubated with an anti-SARS-CoV-2 spike protein primary antibody (provided
167 by Jens Wrarmert, Emory University) conjugated to biotin for 2 hours at room temperature (RT),
168 then washed 3 times. Cells were incubated with an avidin-HRP conjugated secondary antibody

169 for 1 hour at RT. Foci were visualized using True Blue HRP substrate and imaged on an ELI-
170 SPOT reader (CTL Analyzers)²⁴.

171
172 **IFN- α ELISA.** Human IFN- α concentration in cell-culture supernatants was measured by
173 enzyme-linked immunosorbent assay (ELISA; PBL Biomedical Laboratories, Piscataway, NJ)
174 according to the manufacturer's instructions.

175
176 **Quantitative PCR analysis.** pHAE cultures were lysed by adding RNA lysis buffer directly to the
177 apical layer for >5 minutes, then lysate was collected in Eppendorf tubes. RNA was extracted
178 using the Zymo Quick-RNA MiniPrep kit (VWR, R1055) according to the manufacturers protocol,
179 then reverse transcribed into cDNA using a high-capacity cDNA reverse transcription kit (Thermo
180 Fisher, 43-688-13). RNA levels were quantified using the IDT Prime Time Gene Expression
181 Master Mix, and Taqman gene expression Primer/Probe sets. All qPCR was performed in 384-
182 well plates and run on a QuantStudio5 qPCR system. Viral RNA was quantified using SARS-CoV-
183 2 Rdrp specific primers and probes as described in Vanderheiden et al. The following Taqman
184 Primer/ Probe sets were used in this analysis: Gapdh (Hs02758991_g1), IFIT2 (Hs01922738_s1),
185 IFIH1 (Hs00223420_m1). C_T values were normalized to the reference gene GAPDH and
186 represented as fold change over mock.

187
188 **RNA-Sequencing** pDCs were centrifuged and lysis buffer was added to the pellet. RNA was
189 extracted using the RNAeasy microkit (Qiagen) following manufacturer's instructions. RNA from
190 pHAE cells was extracted as described above, and mRNA sequencing libraries were prepared by
191 the Yerkes Genomics Core using the Clontech SMART-Seq v4 kit. Barcoding and sequencing
192 primers were added using a NexteraXT library kit, and validated by microelectrophoresis.

193 Libraries were sequenced on an Illumina NovaSeq 6000 and mapped to the human reference
194 genome 38 using DNASTAR software. Viral genes were mapped to the FDAARGOS_983 strain
195 of the 2019-nCoV/USA-WA1/2020 SARS-CoV-2 isolate. Reads were normalized and differentially
196 expressed genes were analyzed using DESeq2 (Bioconductor). Gene set enrichment analysis
197 was performed using the software provide by the Broad Institute and the MSigDB database. The
198 raw data of all RNA sequencing will be deposited into the Gene Expression Omnibus (GEO)
199 repository and the accession number will be available following acceptance of this manuscript.

200

201 **Statistical analysis.** Statistical analyses were performed using GraphPad Prism 8, ggplot2 R
202 package, and GSEA software. Statistical significance was determined as P value of 0.05 using
203 Student's t test or a one-way analysis of variance (ANOVA). All comparisons were made between
204 treatment or infection conditions with time point-matched, uninfected and untreated controls.

205 **Results**

206 **Plasmacytoid Dendritic cells (pDCs) recognize SARS-CoV-2 and produce type I IFN.** pDCs
207 are uniquely poised to respond to pathogen infection and produce large amounts of type I IFNs.
208 However, the role of pDCs in responding to SARS-CoV-2 is not well understood. To investigate
209 this, pDCs were isolated from blood of healthy donors and infected with SARS-CoV-2. CpG A
210 (ODN2216 at 6 μ g/ml) was used as control. Following SARS-CoV-2 infection, pDCs produced over
211 3500 pg/ml of IFN- α as early as 24 hours post-infection (**Figure 1A**). To determine if virus
212 replication is required for pDCs to respond to SARS-CoV-2, we stimulated pDCs with either live
213 SARS-CoV-2 or UV inactivated SARS-CoV-2 (UV-SARS-CoV-2) at equivalent MOIs and
214 measured IFN- α production. pDCs maintained IFN- α production after stimulation with UV-SARS-
215 CoV-2 as compared to live SARS-CoV-2, demonstrating that virus replication is not required by
216 pDCs for sensing SARS-CoV-2 and to produce type I IFN.

217

218 **Transcriptional profile of SARS-CoV-2 stimulated pDCs shows type I and type III IFN and**
219 **apoptosis signature.** Besides their ability to produce type I IFN, pDCs are able to produce
220 several proinflammatory cytokines and chemokines as well as type III IFN¹⁷. To determine the
221 response of pDCs to SARS-CoV-2, and identify if there are different expression patterns when
222 pDCs are stimulated with SARS-CoV-2 vs. UV-SARS-CoV-2 or CpG, pDCs were stimulated with
223 SARS-CoV-2, UV-SARS-CoV-2 and CpG, RNA was isolated 12h post stimulation and bulk
224 RNAseq performed. pDCs stimulated with either SARS-CoV-2 or UV-SARS-CoV-2 expressed
225 high levels of IFN- β , IFN- α as well as type III IFN: IFN- λ 1 and IFN- λ 3 and IFN- ω . SARS-CoV-2
226 and UV-SARS-CoV-2 stimulated pDCs also highly expressed several chemokines such as
227 CXCL10 (IP-10) and CXCL11 (IP-9) CCL7 (MCP3), CCL8 (MCP2), CCL2 (MCP-1) which recruit
228 monocytes and T cells to sites of inflammation, as well as promote T cell adhesion³². Finally,
229 pDCs also upregulated IDO expression which has been associated with pDC-dependent induction

230 of T regulatory cells (Tregs)^{33,34} (**Figure 2A-C**). When comparing stimulation of pDCs with SARS-
231 CoV-2 to pDCs stimulated with either UV-SARS-CoV-2 or CpG A we confirmed that the type I
232 and III IFN gene expression was similar in all three groups (**Figure 2C and D**). However, there
233 were some DEGs were present only each of the conditions, Interestingly, we also observed an
234 increase in the apoptosis signature in SARS-CoV-2 activated pDCs when compared to medium
235 stimulated pDCs suggesting pDCs may die after activation with SARS-CoV-2 and type I and III
236 IFN production (**Figure 2E**). These results confirm that viral replication is not needed for a high
237 production of type I and type III IFN by pDCs after sensing SARS-CoV-2 infection, and that
238 stimulation with SARS-CoV-2 may increase the apoptosis signature in pDCs.

239

240 **pDCs protect primary human airway epithelial (pHAE) cells from SARS-CoV-2 infection.**

241 Since pDCs are able to produce type I and III IFN after SARS-CoV-2 stimulation, we next
242 investigated if pDC-derived-IFN is able to control SARS-CoV-2 replication and protect lung
243 epithelial cells. To test this, we utilized pHAE cells isolated from the bronchial or tracheal
244 region of healthy donors. These cells are cultured in an air-liquid interface to create a
245 polarized, pseudostratified epithelial layer that models the critical features of the human
246 respiratory tract, such as cilium movement and mucus production³¹. We have previously
247 shown that pHAE cells are susceptible to SARS-CoV-2 infection, and respond by producing
248 a variety of inflammatory cytokines³⁵. However, SARS-CoV-2 infection does not induce the
249 production of type I or type III IFN by pHAE cells. To test if pDCs are able to control viral
250 infection in pHAE cells, we developed a co-culture system. pHAE cells were infected with
251 SARS-CoV-2 at MOI=1 for 1 hour. In parallel, pDCs were stimulated with UV-SARS-CoV-2,
252 CpG A, or left untreated. After 3 hours, pDCs were washed and placed in the bottom well of
253 the SARS-CoV-2 infected-pHAE transwell culture (**Figure 3A**). Addition of recombinant IFN-

254 β , UV-SARS-CoV-2 and CpG A to the bottom wells in the absence of pDCs was used as
255 control. UV-SARS-CoV-2 stimulated pDCs and CpG stimulated pDCs were able to strongly
256 reduce replication and virus production of SARS-CoV-2 in pHAE cells. Co-culture with
257 stimulated pDCs reduced infectious SARS-CoV-2 production (as measured by focus-forming
258 assay) from the apical surface of pHAE cells by 1000-fold, as well as viral RNA (100-fold
259 reduction) at 72h post infection (**Figure 3B and C**). Importantly, the protective effect was
260 mediated by pDCs, since addition of CpG or UV-SARS-CoV-2 alone to the basolateral side
261 didn't reduce viral replication. Interestingly, unstimulated pDCs were also able to reduce the
262 viral load, suggesting that infected pHAE cells are able to activate a type I IFN response in
263 pDCs that is rapid enough to decrease viral replication within 72 hours (**Figure 3B and C**).
264 As seen in our previous study, addition of IFN- β to the bottom well reduced viral replication,
265 confirming its protective effect against SARS-CoV-2 and suggesting pDCs act through type I
266 IFN production. Indeed, when we analyzed the transcriptional profile of infected pHAEs co-
267 cultured with pDCs we observed the upregulation of several interferon-stimulated genes
268 (ISGs) such as IFIH1 and IFIT2 (**Figure 3D**).

269

270 **Activated pDCs induce an antiviral profile in SARS-CoV-2 pHAE infected cells.** We next
271 evaluated how the presence of activated pDCs changes the transcriptional profile of SARS-
272 CoV-2 infected pHAE cells. To this end, we performed mRNAseq analysis of pHAE cells
273 infected with SARS-CoV-2 and co-cultured with pDCs, UV-SARS-CoV-2 activated pDCs, and
274 IFN- β or media as controls. First, analysis at 72 hrs post infection showed a reduction in viral
275 read counts spanning the whole viral genome when infected pHAEs cells were co-cultured
276 with activated pDCs. Interestingly, co-culture with activated pDCs was more efficient than

277 addition of IFN- β in reducing viral RNAs, which is likely due to the concerted action of type I
278 IFN (IFN- β and IFN- α) and type III IFN (IFN- λ) produced by pDCs (Figure 4A).

279 To determine if the presence of activated pDCs in the co-culture changed the response of
280 pHAE cells to infection, we plotted fold-change over mock for each co-culture condition (IFN-
281 β treatment, pDC alone, UV-Cov-2+pDC) to the untreated infected control. Investigation of
282 the differentially expressed genes (DEGs; cutoffs: $p < 0.01$ fold change $< > 2$) in infected pHAE
283 cells treated with IFN- β treated cells or untreated identified that many DEGs were expressed
284 in both conditions (112, yellow), but IFN- β treatment induced 242 uniquely expressed genes
285 (green) while untreated cells only had 12 unique DEGs (red) (**Figure 4B**). Comparison of
286 untreated pHAEs with pDC co-cultured pHAEs resulted in similar numbers of DEGs
287 expressed by both or only untreated cells, however pDC co-cultured cells had 448 (green)
288 unique DEGs. Co-culture with UV-CoV-2 stimulated pDCs resulted in the exact same number
289 of DEGs expressed in both or only untreated cells, however there were three times more
290 (1518 genes) genes uniquely expressed in co-cultured pHAEs when the pDCs were
291 stimulated with UV-CoV-2 as compared to unstimulated pDCs (**Figure 4B**). This analysis
292 determined that 1,518 genes were differentially expressed only if pHAEs cells were co-
293 cultured with activated pDCs (**Figure 4B**). These results suggest that the presence of
294 activated pDCs profoundly change the response of pHAEs to infection.

295

296 We next investigated the identity of the unique DEGs induced by co-culture of infected pHAE
297 cells with pDCs. As expected, IFN- β induced expression of key signaling molecules and
298 transcription factors in the type I IFN pathway such as STAT1 and IRF7. However, co-culture
299 of pHAE cells with unstimulated pDCs or UV-CoV-2-stimulated pDCs had an even greater
300 upregulation of STAT1 and IRF7 (**Figure 4C**). Accordingly, heatmap analysis identified an

301 upregulation of many ISGs (IFIT2, RSAD2, ISG20) in IFN- β treated, pDC or UV-CoV-2-pDC
302 co-cultured pHAE cells, with not only higher magnitude but also greater breadth of ISG
303 expression in the pDC co-cultured cells (**Figure 4D**). We also analyzed if pDC co-culture
304 affected the inflammatory response induced in pHAE by SARS-CoV2 infection. As seen in
305 figure 4D, co-culture with pDCs increased the inflammatory response of infected pHAE cells.
306 Additionally, co-culture with UV-CoV-2-pDC upregulated the expression of 10 key
307 inflammatory response genes, such as cytokine receptors IL12RB1, IL15RA, CSF3R, that
308 was not observed in untreated, or IFN β treated pHAE cells. Interestingly, co-culture with pDCs
309 also induced the expression of molecules of the antigen presentation pathway. This may be
310 of particular importance during the initial phases of infection in order harness the adaptive
311 immune response to SARS-CoV-2.

312

313 Discussion

314 In this study, we show that pDCs are able to recognize SARS-CoV-2 infection and produce
315 high levels of type I IFN. Activated pDCs are able to control SARS-CoV-2 infection in pHAE
316 cells by inducing an interferon response and an antiviral transcriptional program. SARS-CoV-
317 2 and other coronaviruses are able to avoid recognition and type I IFN induction in several
318 cell populations including airway epithelial cells. However, pDCs are able to sense SARS-
319 CoV-2 and produce large amounts of type I and type III interferons. One major difference
320 between pDCs and other cells is their expression of TLRs such as TLR7 which allows them
321 to sense ssRNA¹⁷. Indeed, when we stimulated pDCs with UV-inactivated SARS-CoV-2
322 similar to live SARS-CoV-2, they produced IFN- α , suggesting that pDCs do not require active
323 infection to sense the presence of SARS-CoV-2. A recent report has also shown that pDCs
324 can get activated and upregulate CD80, CD86, CCR7 and OX40 after stimulation with SARS-
325 CoV-2 independently of viral replication³⁶. This gives pDCs two unique advantages for viral
326 sensing: they are able to rapidly recognize the presence of viral RNA even before viral
327 replication would start, without being susceptible to infection. Moreover, if pDCs don't support
328 productive SARS-CoV-2 replication, they may not be susceptible to the IFN antagonist effects
329 of several SARS-CoV-2 nonstructural proteins.

330

331 We used human pHAE cell cultures to model the epithelial cell layer of the respiratory tract.
332 pHAEs are susceptible to SARS-CoV-2 infection and recapitulate several features of
333 respiratory disease, including inflammatory cytokine release and enrichment of ER stress
334 pathways²⁴. Co-culture of SARS-CoV-2 infected pHAEs together with pDCs that have been
335 stimulated with UV-SARS-CoV-2 resulted in inhibition of viral particle production as seen by
336 the reduction of viral titers in focus-forming assays (FFA) of the apical side of the pHAEs and

337 inhibition of viral replication as seen in the reduction of viral RNA in the cells. Interestingly,
338 co-culture of unstimulated pDCs with infected pHAE cells also resulted in reduced viral titers.
339 We have previously demonstrated that viral particles are only released to the apical side of
340 the pHAE culture²⁴. Moreover, we confirmed the absence of infectious virus in the basolateral
341 medium, where pDCs were located, by FFA. Nevertheless, pDCs were able to sense the
342 infection of pHAE cells. Future studies will be needed to investigate if pDCs recognize viral
343 RNA or soluble mediators from infected pHAE cells in the basolateral side.

344

345 The transcriptional analysis of SARS-CoV-2 infected pHAE cells corroborated that they are
346 unable to produce type I IFN, although they can produce several inflammatory cytokines²⁴.
347 However, when infected pHAEs were co-cultured with activated pDCs, a set of 1510
348 additional genes were upregulated when compared to infected pHAEs that were not co-
349 cultured with pDCs, revealing the strong impact of the presence of pDCs in pHAE cell
350 response to viral infection. Several of these uniquely upregulated genes are ISGs or have
351 been shown to have an antiviral role in the control of coronavirus infections, for example OAS
352 or IFIT. Interestingly, the expression in pHAEs of genes upregulated by inflammatory
353 cytokines increased by the presence of pDCs, suggesting that pDC production of
354 inflammatory cytokines enhances the inflammatory response of pHAEs. We also observed
355 the upregulation of genes involved in the antigen presentation pathway, which were not
356 upregulated in the infected pHAE cells without pDCs. A key role of type I IFN signaling is the
357 upregulation of class I antigen presentation to allow cytotoxic T cells to recognize viral
358 infected cells and eliminate them. This is an additional mechanism by which pDC-derived IFN
359 may contribute to viral control and induction of the adaptive immune response.

360

361 Since pDCs are able to sense SARS-CoV-2 infection and reduce viral replication, the
362 remaining question is, how can SARS-CoV-2 overcome pDC recognition to establish
363 infection. Previous studies have demonstrated that the frequency of pDCs in the blood of
364 hospitalized Covid-19 patients is much lower than the frequencies in healthy donors⁹. This
365 may be the result of three different mechanisms: pDCs may be activated very early on during
366 infection, and in individuals where infection is more severe we observe the loss of the
367 previously activated pDCs. A study by Swiecki et al. showed that pDCs die by apoptosis after
368 viral recognition and IFN- α production³⁷. Consistently, we observed an increase in the
369 apoptosis signature in SARS-CoV-2 stimulated pDCs. Moreover, it has been also shown that
370 during prolonged or chronic viral infections, pDCs present an exhausted phenotype and stop
371 producing type I IFN^{38,39}. Another possibility is that SARS-CoV-2 viral proteins directly target
372 pDCs *in vivo* and result in their depletion. Network analyses of single-cells RNA seq of COVID-
373 19 patients showed an association between apoptosis in pDCs and disease severity²². Finally, it
374 is also possible that pDCs are largely recruited to the infected tissues such as lungs and this
375 results in reduced frequencies in peripheral blood. Indeed, numbers of pDCs are found in the
376 BAL of mild COVID-19 patients in contrast to severe COVID-19 patients which have reduced
377 numbers of pDCs in BAL¹⁰. Future studies in animal models, where the initial hours after
378 infection can be studied will be very helpful in elucidating the fate of pDCs and why they are
379 reduced in COVID-19 patients. Recently, a study in which Covid-19 patients were treated with
380 IFN showed that early interferon treatment associates with favorable clinical response in
381 COVID-19 patients¹⁵. Here we showed that co-culture of pDCs with infected pHAEs was
382 better at controlling SARS-CoV-2 infection than pre-treatment of pHAEs with IFN- β ,
383 suggesting a potential use of pDC activation as treatment for COVID-19. Since pDCs are
384 able to produce not only IFN- β , but IFN- α , and IFN- λ , rescuing pDC numbers or activating

385 the remaining pDCs in COVID-19 patients is an attractive strategy to reduce the severity of
386 the disease.

387

388 **Figure legends**

389 **Figure 1. Plasmacytoid dendritic cells (pDCs) recognize SARS-CoV-2 and produce IFN-**

390 **α .** A) human pDCs were mock infected (media), infected with SARS-CoV-2 (MOI=1) or
391 stimulated with CpG A (6 μ g/ml) for 24 or 48 hr. B) human pDCs were stimulated with medium,
392 SARS-CoV-2, UV inactivated SARS-CoV-2 or CpG A for 24h. At the indicated timepoints
393 supernatants were collected and IFN- α was measured by ELISA. Dots represent pDCs from
394 single donors, bars depict means. Graphs are representative of 3 independent experiments.
395 Data was analyzed using one-way ANOVA ***, P<0.001.

396

397 **Figure 2. pDC transcriptional profile shows a type I and type II IFN signature after**

398 **SARS-CoV-2 stimulation.** Human pDCs were infected with SARS-CoV-2 (MOI=1) or
399 stimulated with UV-SARS-CoV-2 (MOI=1), CpG A (6 μ g/ml) or medium. After 12h cells were
400 collected for bulk-RNA-Seq analysis. A) Volcano plot showing all differentially regulated
401 genes (DEG) between media and SARS-CoV-2 infected pDCs in red and blue. B) GSEA plot
402 showing enrichment in interferon-alpha-response genes after SARS-CoV-2 activation in
403 pDCs. C) Heatmap illustrating the z-scores for the 30 most differentially upregulated genes
404 in SARS-CoV-2 infected pDCs. D) Fold-change vs fold-change plot of SARS-CoV-2 vs
405 medium and UV-SARS-CoV-2 vs medium showing in green the DEG in SARS-CoV-2
406 only, in red the DEG in SARS-CoV-2 only and in orange the DEG in both conditions and
407 change vs fold-change plot of SARS-CoV-2 vs medium and CpG A vs medium showing in
408 green the DEG in CpG only, in red the DEG in SARS-CoV-2 only and in orange the DEG in
409 both conditions. E) GSEA plot showing enrichment in Apoptosis genes in medium vs SARS-
410 CoV-2 stimulated pDCs.

411 **Figure 3. pDCs reduce SARS-CoV-2 replication in pHAE cultures.** A) Experimental
412 schematic. B) pDCs were stimulated for 3 hours in complete RPMI supplemented with; medium,
413 CpG A (ODN2216 at 6 μ g/ml), or UV inactivated SARS-CoV-2 (MOI=1) at 37°C. In parallel,
414 differentiated pHAE cultures were infected with SARS-CoV-2 (MOI=1). After 3 hours the
415 basolateral media was replaced with fresh media containing the stimulated pDCs, medium only,
416 or IFN β (100 IU/mL). After 72 hours, the apical side was washed and supernatant was collected
417 and pHAE cells were harvested and RNA extracted. B) Viral titers in the apical side, C) Total viral
418 RNA in the cells and D) IFIH1 and IFIT2 expression in pHAEs in the different conditions tested.
419 Dots represent single replicates and bars represent the means. Data was analyzed using one-
420 way ANOVA. *, P<0.05; **, P<0.01; ***, P<0.001.

421

422 **Figure 4. pDCs induce an interferon signature in pHAE cells.** Bulk RNA-seq analysis was
423 performed in pHAE cells from the co-culture experiment described in figure 3. A) Normalized read
424 counts (log₂) of SARS-CoV-2 RNA products, using the MT246667.1 reference sequence. B)
425 Fold-change vs fold-change plot of SARS-CoV-2 infected pHAE cells vs uninfected pHAE
426 cells and SARS-CoV-2 infected pHAE cells treated with IFN- β vs uninfected pHAE cells. Fold-
427 change vs fold-change plot of SARS-CoV-2 infected pHAE cells vs uninfected pHAE cells
428 and SARS-CoV-2 infected pHAE cells co-cultured with UV-SARS-CoV-2 treated pDCs vs
429 uninfected pHAE and fold-change vs fold-change plot of SARS-CoV-2 infected pHAE cells vs
430 uninfected pHAE cells and SARS-CoV-2 infected pHAE cells co-cultured with pDCs vs
431 uninfected pHAE cells. Dots highlighted in green, red and orange are the DEG in each
432 condition. C) Normalized read counts (log₂) of expression of STAT1 and IRF7 in pHAE cells
433 treated in the indicated conditions. D) Heatmap illustrating the z-scores for genes associated
434 to the interferon response, inflammatory response and antigen presentation. Dots represent

435 single replicates and bars represent the means. Data was analyzed using one-way ANOVA. *,
436 $P < 0.05$; **, $P < 0.01$; ***, $P < 0.001$.

437

438

439

440

441

442 **Funding:** This work was supported in part by grants (HHSN272201400004C (M.S.S.), U19
443 AI090023 (M.S.S.), P51 OD011132 and R56 AI147623 (to Emory University) from the National
444 Institute of Allergy and Infectious Diseases, National Institutes of Health, COVID-Catalyst-
445 I³ Funds from the Woodruff Health Sciences Center and Emory School of Medicine made possible
446 through a grant from the O. Wayne Rollins Foundation, and through the Georgia CTSA NIH
447 award **UL1-TR002378** (L.C-B and M.S.S.), the Emory Executive Vice President for Health
448 Affairs Synergy Fund award, the Pediatric Research Alliance Center for Childhood Infections and
449 Vaccines and Children's Healthcare of Atlanta, Center for Childhood Infections and Vaccines
450 Special Coronavirus Pilot award, the Emory-UGA Center of Excellence for Influenza Research
451 and Surveillance, and Woodruff Health Sciences Center 2020 COVID-19 CURE Award. The
452 Yerkes NHP Genomics Core is supported in part by NIH P51 OD011132, and an equipment
453 grant, NIH S10 OD026799. The funders had no role in study design, data collection and
454 analysis, decision to publish, or preparation of the manuscript.

455

456 **Author contributions:**

457 L. C-B., and M.S. contributed to the acquisition, analysis, and interpretation of the data, as
458 well as the conception and design of the study, and wrote the manuscript A.V. contributed
459 to the acquisition, analysis, and interpretation of the data, and wrote the manuscript. C.J.R.,
460 P.R, M.D-G., and T.C. contributed to the acquisition and analysis of the data, L.J.A. and
461 A.G. contributed to the interpretation of the data.

462

463 **Declaration of interests:** The authors declare no competing interest

464 References

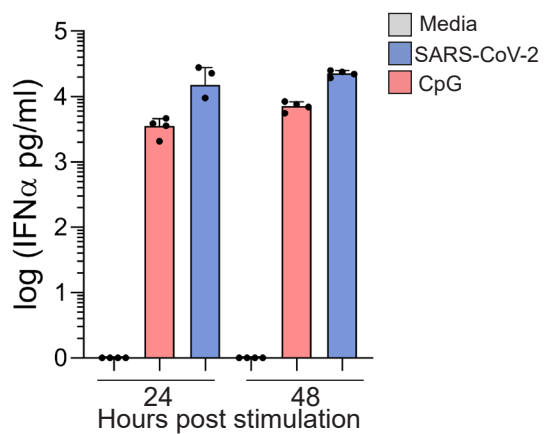
- 465 1 Zhou, P. *et al.* A pneumonia outbreak associated with a new coronavirus of probable bat
466 origin. *Nature* **579**, 270-273, doi:10.1038/s41586-020-2012-7 (2020).
- 467 2 Zhu, N. *et al.* A Novel Coronavirus from Patients with Pneumonia in China, 2019. *N Engl*
468 *J Med* **382**, 727-733, doi:10.1056/NEJMoa2001017 (2020).
- 469 3 Lazear, H. M., Schoggins, J. W. & Diamond, M. S. Shared and Distinct Functions of Type
470 I and Type III Interferons. *Immunity* **50**, 907-923, doi:10.1016/j.immuni.2019.03.025
471 (2019).
- 472 4 Blanco-Melo, D. *et al.* Imbalanced Host Response to SARS-CoV-2 Drives Development
473 of COVID-19. *Cell* **181**, 1036-1045 e1039, doi:10.1016/j.cell.2020.04.026 (2020).
- 474 5 Kindler, E. & Thiel, V. SARS-CoV and IFN: Too Little, Too Late. *Cell Host Microbe* **19**,
475 139-141, doi:10.1016/j.chom.2016.01.012 (2016).
- 476 6 Kindler, E., Thiel, V. & Weber, F. Interaction of SARS and MERS Coronaviruses with the
477 Antiviral Interferon Response. *Adv Virus Res* **96**, 219-243,
478 doi:10.1016/bs.aivir.2016.08.006 (2016).
- 479 7 Totura, A. L. & Baric, R. S. SARS coronavirus pathogenesis: host innate immune
480 responses and viral antagonism of interferon. *Curr Opin Virol* **2**, 264-275,
481 doi:10.1016/j.coviro.2012.04.004 (2012).
- 482 8 Kindler, E. & Thiel, V. To sense or not to sense viral RNA--essentials of coronavirus innate
483 immune evasion. *Curr Opin Microbiol* **20**, 69-75, doi:10.1016/j.mib.2014.05.005 (2014).
- 484 9 Arunachalam, P. S. *et al.* Systems biological assessment of immunity to mild versus
485 severe COVID-19 infection in humans. *Science* **369**, 1210-1220,
486 doi:10.1126/science.abc6261 (2020).
- 487 10 Liao, M. *et al.* Single-cell landscape of bronchoalveolar immune cells in patients with
488 COVID-19. *Nat Med* **26**, 842-844, doi:10.1038/s41591-020-0901-9 (2020).
- 489 11 Schulte-Schrepping, J. *et al.* Severe COVID-19 Is Marked by a Dysregulated Myeloid Cell
490 Compartment. *Cell* **182**, 1419-1440 e1423, doi:10.1016/j.cell.2020.08.001 (2020).
- 491 12 Bastard, P. *et al.* Autoantibodies against type I IFNs in patients with life-threatening
492 COVID-19. *Science* **370**, doi:10.1126/science.abd4585 (2020).
- 493 13 Zhang, Q. *et al.* Inborn errors of type I IFN immunity in patients with life-threatening
494 COVID-19. *Science* **370**, doi:10.1126/science.abd4570 (2020).
- 495 14 Levy, R. *et al.* IFN- α 2a Therapy in Two Patients with Inborn Errors of TLR3 and IRF3
496 Infected with SARS-CoV-2. *J Clin Immunol* **41**, 26-27, doi:10.1007/s10875-020-00933-0
497 (2021).
- 498 15 Wang, N. *et al.* Retrospective Multicenter Cohort Study Shows Early Interferon Therapy
499 Is Associated with Favorable Clinical Responses in COVID-19 Patients. *Cell Host Microbe*
500 **28**, 455-464 e452, doi:10.1016/j.chom.2020.07.005 (2020).
- 501 16 Reizis, B. Plasmacytoid Dendritic Cells: Development, Regulation, and Function.
502 *Immunity* **50**, 37-50, doi:10.1016/j.immuni.2018.12.027 (2019).

- 503 17 Swiecki, M. & Colonna, M. The multifaceted biology of plasmacytoid dendritic cells. *Nat*
504 *Rev Immunol* **15**, 471-485, doi:10.1038/nri3865 (2015).
- 505 18 Kadowaki, N. *et al.* Subsets of human dendritic cell precursors express different toll-like
506 receptors and respond to different microbial antigens. *J Exp Med* **194**, 863-869,
507 doi:10.1084/jem.194.6.863 (2001).
- 508 19 Kumagai, Y. *et al.* Cutting Edge: TLR-Dependent viral recognition along with type I IFN
509 positive feedback signaling masks the requirement of viral replication for IFN- α
510 production in plasmacytoid dendritic cells. *J Immunol* **182**, 3960-3964,
511 doi:10.4049/jimmunol.0804315 (2009).
- 512 20 Cervantes-Barragan, L. *et al.* Control of coronavirus infection through plasmacytoid
513 dendritic-cell-derived type I interferon. *Blood* **109**, 1131-1137, doi:10.1182/blood-2006-05-
514 023770 (2007).
- 515 21 Cervantes-Barragan, L. *et al.* Plasmacytoid dendritic cells control T-cell response to
516 chronic viral infection. *Proc Natl Acad Sci U S A* **109**, 3012-3017,
517 doi:10.1073/pnas.1117359109 (2012).
- 518 22 Liu, C. *et al.* Time-resolved systems immunology reveals a late juncture linked to fatal
519 COVID-19. *Cell* **184**, 1836-1857 e1822, doi:10.1016/j.cell.2021.02.018 (2021).
- 520 23 Hao, S. *et al.* Long-Term Modeling of SARS-CoV-2 Infection of In Vitro Cultured Polarized
521 Human Airway Epithelium. *mBio* **11**, doi:10.1128/mBio.02852-20 (2020).
- 522 24 Vanderheiden, A. *et al.* Type I and Type III Interferons Restrict SARS-CoV-2 Infection of
523 Human Airway Epithelial Cultures. *J Virol* **94**, doi:10.1128/JVI.00985-20 (2020).
- 524 25 Lieberman, N. A. P. *et al.* In vivo antiviral host transcriptional response to SARS-CoV-2
525 by viral load, sex, and age. *PLoS Biol* **18**, e3000849, doi:10.1371/journal.pbio.3000849
526 (2020).
- 527 26 Fiege, J. K. *et al.* Single cell resolution of SARS-CoV-2 tropism, antiviral responses, and
528 susceptibility to therapies in primary human airway epithelium. *PLoS Pathog* **17**,
529 e1009292, doi:10.1371/journal.ppat.1009292 (2021).
- 530 27 Rebendenne, A. *et al.* SARS-CoV-2 triggers an MDA-5-dependent interferon response
531 which is unable to control replication in lung epithelial cells. *J Virol*, doi:10.1128/JVI.02415-
532 20 (2021).
- 533 28 Lokugamage, K. G. *et al.* Type I Interferon Susceptibility Distinguishes SARS-CoV-2 from
534 SARS-CoV. *J Virol* **94**, doi:10.1128/JVI.01410-20 (2020).
- 535 29 Felgenhauer, U. *et al.* Inhibition of SARS-CoV-2 by type I and type III interferons. *J Biol*
536 *Chem* **295**, 13958-13964, doi:10.1074/jbc.AC120.013788 (2020).
- 537 30 Xie, X. *et al.* An Infectious cDNA Clone of SARS-CoV-2. *Cell Host Microbe* **27**, 841-848
538 e843, doi:10.1016/j.chom.2020.04.004 (2020).
- 539 31 Chirkova, T. *et al.* CX3CR1 is an important surface molecule for respiratory syncytial virus
540 infection in human airway epithelial cells. *J Gen Virol* **96**, 2543-2556,
541 doi:10.1099/vir.0.000218 (2015).

- 542 32 Rot, A. & von Andrian, U. H. Chemokines in innate and adaptive host defense: basic
543 chemokines grammar for immune cells. *Annu Rev Immunol* **22**, 891-928,
544 doi:10.1146/annurev.immunol.22.012703.104543 (2004).
- 545 33 Boasso, A. *et al.* HIV inhibits CD4+ T-cell proliferation by inducing indoleamine 2,3-
546 dioxygenase in plasmacytoid dendritic cells. *Blood* **109**, 3351-3359, doi:10.1182/blood-
547 2006-07-034785 (2007).
- 548 34 Sharma, M. D. *et al.* Plasmacytoid dendritic cells from mouse tumor-draining lymph nodes
549 directly activate mature Tregs via indoleamine 2,3-dioxygenase. *J Clin Invest* **117**, 2570-
550 2582, doi:10.1172/JCI31911 (2007).
- 551 35 Vanderheiden, A. *et al.* Type I and Type III IFN Restrict SARS-CoV-2 Infection of Human
552 Airway Epithelial Cultures. 2020.2005.2019.105437, doi:10.1101/2020.05.19.105437 %J
553 bioRxiv (2020).
- 554 36 Onodi, F. *et al.* SARS-CoV-2 induces human plasmacytoid predendritic cell diversification
555 via UNC93B and IRAK4. *J Exp Med* **218**, doi:10.1084/jem.20201387 (2021).
- 556 37 Swiecki, M. *et al.* Type I interferon negatively controls plasmacytoid dendritic cell numbers
557 in vivo. *J Exp Med* **208**, 2367-2374, doi:10.1084/jem.20110654 (2011).
- 558 38 Macal, M. *et al.* Self-Renewal and Toll-like Receptor Signaling Sustain Exhausted
559 Plasmacytoid Dendritic Cells during Chronic Viral Infection. *Immunity* **48**, 730-744 e735,
560 doi:10.1016/j.immuni.2018.03.020 (2018).
- 561 39 Zuniga, E. I., Liou, L. Y., Mack, L., Mendoza, M. & Oldstone, M. B. Persistent virus infection
562 inhibits type I interferon production by plasmacytoid dendritic cells to facilitate
563 opportunistic infections. *Cell Host Microbe* **4**, 374-386, doi:10.1016/j.chom.2008.08.016
564 (2008).
- 565

Figure 1

A.



B.

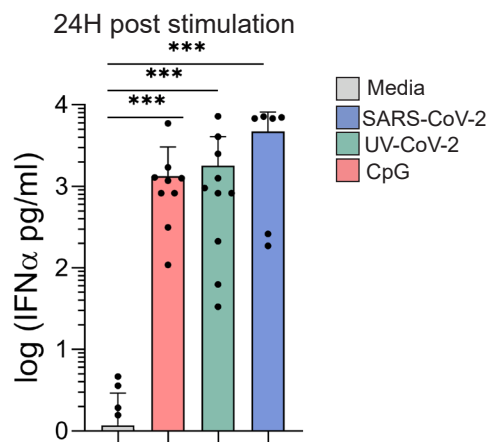
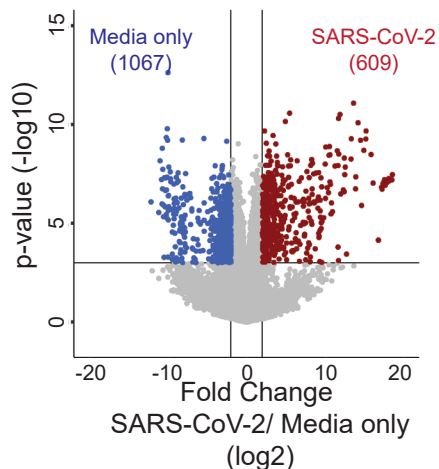
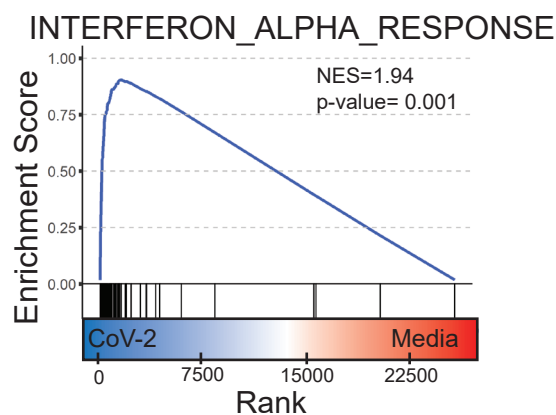


Figure 2

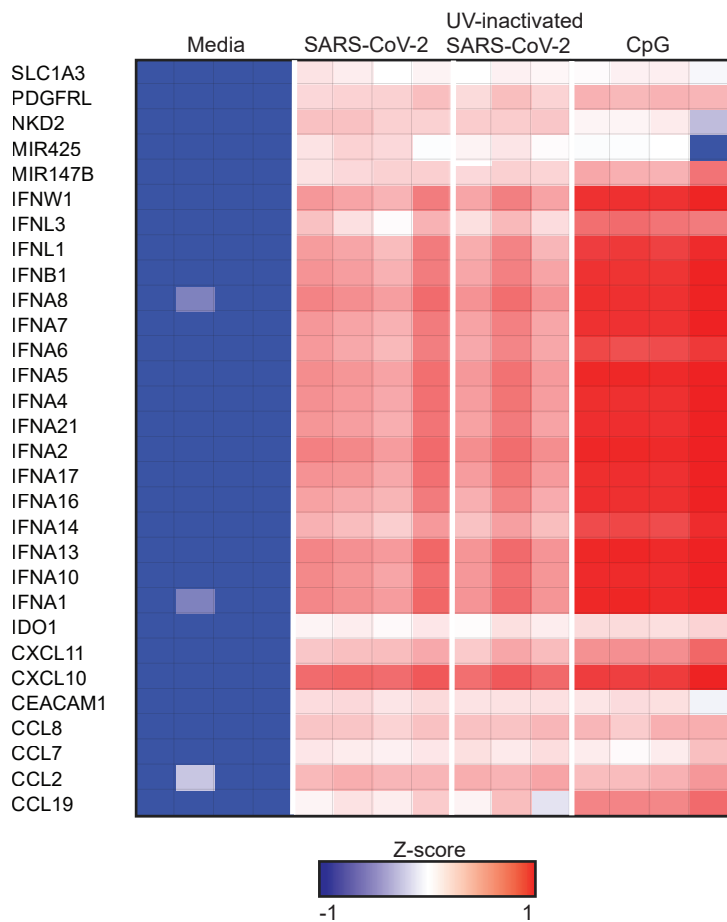
A.



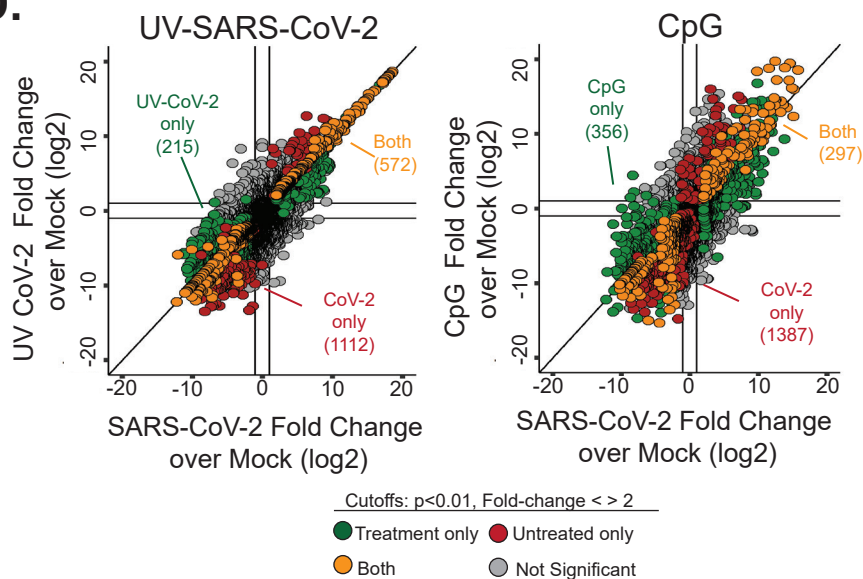
B.



C.



D.



E.

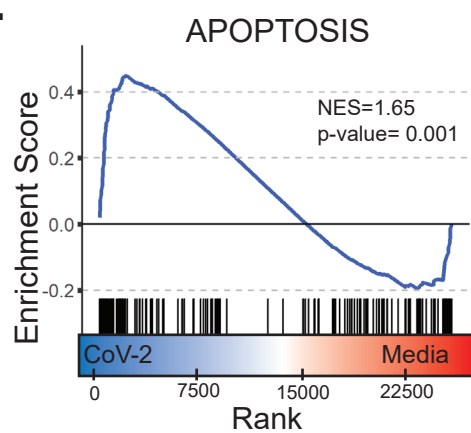
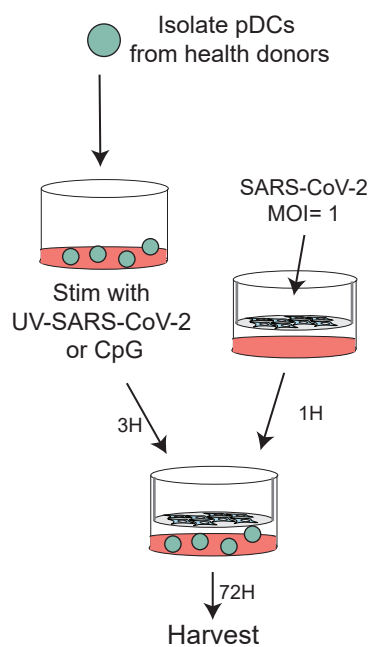
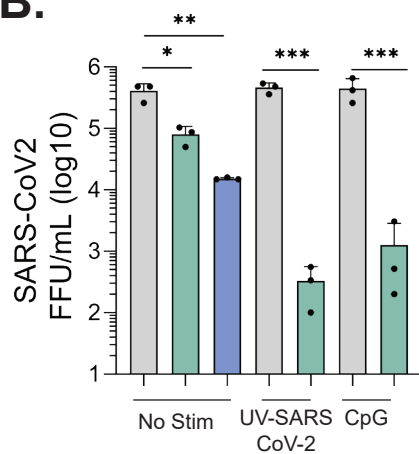


Figure 3

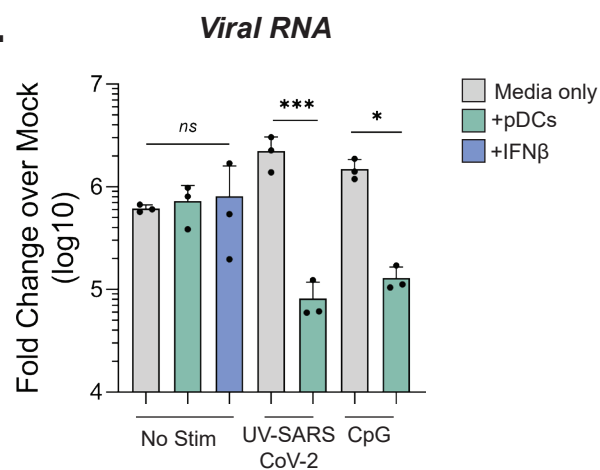
A.



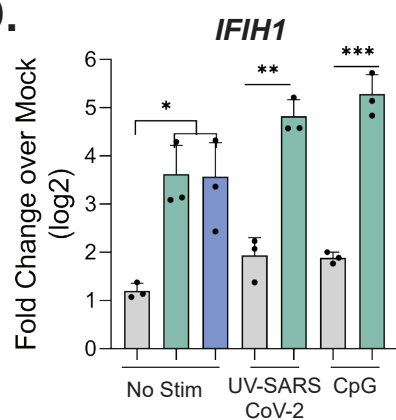
B.



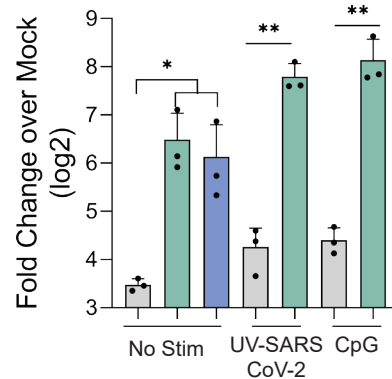
C.



D.



IFI1



IFIT2

